ZIGBEE-ENABLED AI-BASED PULSE OXIMETER FOR ACCURATE DETECTION OF HYPOXEMIA AND OTHER CONTAGIOUS DISEASES IN NIGERIA AND BEYOND

BY

IDRIS MUSA

(Principal Investigator)
(im4idrismusa@yahooco.uk, **+234(0)8145512666**)

A Proposal Submitted to The National Agency for Science and Engineering Infrastructure (NASENI)

OCTOBER, 2025

SECTION ONE

INTRODUCTION

1.1 Background of the Research

The recent outbreak of the Corona Virus Disease of 2019 (COVID-19) and other contagious global pandemics sparked up many concerns on the need to develop effective measures in order to combat the menace of this devastating disease. These measures are to be aimed at minimizing the mortality rate amongst victims as well as the medical practitioners (Panneer *et al.*, 2022). One of the effective approaches that have been envisaged to be most suitable for this intended purpose is the development of efficient medical devices that can be used to aid the early detection of symptoms of the viral infection. Due to this fact, the development of an easy to use medical device for this purpose has been a top notch venture in recent decades (Liu *et al.*, 2020).

The reliability of measurements derived from the use of these medical devices is of pertinent importance as these measurements will in turn be used as yardstick for medical prescriptions. So far, there have been myriads of algorithms used for the purpose of calibration of the pulse oximeter design. These algorithms were developed with the aim of mitigating errors due to artefacts which negatively impacts the accuracy of the measurements (Tarvirdizadeh *et al.*, 2020). However, these algorithms often come with their downsides in that while an algorithm may be efficient in mitigating the effects of some external factors, it may not be a best fit in the correction of the problems associated with other factors.

An artefact is an unwanted interference, which has the capacity to alter the accuracy of biomedical signals. A distorting artifact may arise because of the movement of the body part when obtaining the oximetry reading of the patient under consideration. It can also be introduced into the system due to the surrounding bioelectrical signals from neighboring tissues as well as some other external environmental factors (Jiang *et al.*, 2019). Many researchers have proposed different filtering techniques and algorithms to reduce the introduction of errors in the biomedical signals obtained from existing pulse oximeter. Some of these techniques include: Exponential Moving Average (EMA), Savitzky-Golay Filter (SGF), Independent Component Analysis (ICA), Discrete Kalman filter (DKF) etc. (Chugh & Akula, 2018). However, the computational complexity of these algorithms increases the processing time as well as the overhead of the biomedical signal acquisition. Efforts in this area aimed at improving the performance of the existing models abounds. To this end, this project intends to extend the development and commercialization of Artificial Intelligence (AI)-based pulse oximeter which is able to mitigate the problem of varying environmental factors affecting the reliability of performance of the pulse oximeter.

1.2 Significance of the Research

Based on the statistical records of the research conducted by (Bandyopadhyay *et al.*, 2020), it stated that over a hundred and fifty thousand infections was recorded amongst the medical practitioners world-wide. This is especially seen during the early phases of the outbreak of the novel COVID-19 pandemic. These figures was projected to be more during the long run and this is just a particular case of the health risk posed to medical practitioners during the event of an outbreak of an infectious disease. With the trend of events, chances are that there can be an outbreak of other infectious diseases in the future. Because of all these underlining facts, the significance of this research work is geared towards combating the ensuing colossal damage occasioned by the disease which has already lead to the loss of many lives including those of the medical practitioners who in an attempt to rescue the victims of the disease, end up becoming the victims themselves. Thus, this research work seeks to develop an efficient and reliable medical device that can help assist medical practitioners in reducing the risk of exposure to infectious diseases in the event of an outbreak. So far, many working models of the pulse oximeter device is in use but most often than not, error of measurement due to distorting external factors, often affects the quality of the bionic signals measured by the pulse oximeter device and this is what forms major focus of this research.

1.3 Problem Statement

With the emergence of the Covid19 pandemic as well as other infectious diseases, it has become imperative to adopt a pragmatic approach in combating the spread of these diseases (Cesari & Proietti, 2020). One of the ultimate targets of the corona virus as well as other respiratory related diseases is to attack the human lungs thereby making it difficult for the victim to breath. If this process continues without prompt measures taken, soon the level of oxygenated hemoglobin in the patient's blood begins to deplete appreciably, leading to asphyxiation and consequent death of the patient (Chen *et al.*, 2020). In order to carry out medical diagnosis of these respiratory diseases, a pulse oximeter is used to estimate the Saturated Peripheral Oxygen SpO_2 and the Pulse Rate of patients in a medical ward.

However, the quality of the measurement obtained using a pulse oximeter is affected by environmental artefacts such as variations in the ambient light and temperature. To this end, this research work developed an adaptive algorithm to mitigate the impact of the variations in the ambient light and temperature conditions of the surrounding environment for which the proposed design is deployed for use. This was achieved by measuring the ambient light and temperature of the surrounding environment and using the values obtained to compensate for the error in measurement. This was made possible through the use of mathematical model equation that encapsulates the effect of both the variation in ambient light and temperature to enhance the performance of the pulse oximeter device as compared to the model used by the work of (Metcalfe *et al.,* 2021) which was adopted as the base paper for this research work.

1.4 Aim and Objectives

The aim of this project work is to develop a Zigbee enhanced AI-based pulse oximeter to mitigate the effect of varying ambient light and temperature conditions on the accuracy and reliability of SpO_2 and Pulse Rate measurements, which will be incorporated into the design of a locally made prototype and commercialized.

The stated aim will be achieved through the following objectives:

1) To design and implement a ZigBee-enabled, microcontroller-based pulse oximeter system for reliable, real-time monitoring of peripheral oxygen saturation (SpO_2) and pulse rate.
2) To develop a user-friendly App that integrate a Random Forest-based adaptive Machine Learning (ML) algorithm for remote detection and accurate analysis of hypoxemia.
3) To validate and commercialize the proposed system by benchmarking its SpO_2 and pulse rate measurements against those from a clinical-grade pulse oximeter using Mean Absolute Error (MAE) and Root Mean Square Error (RMSE) as performance metrics.

SECTION TWO
LITERATURE REVIEW

2.1 Introduction

The major components of this section of the research comprises of the review of the fundamental concepts and the review of similar works. In the review of fundamental concepts, the available theoretical framework in this area of research is studied. Here, the research explores the significance of these theoretical frame works as it applies to the feasibility of the conduct of this research. After this, the research zooms in on the review of similar works in order to establish the available research gaps which the research intends to use as a base line for justification of the contributions made to the already existing body of knowledge on this area of interest.

2.2 Review of Fundamental Concepts

This subsection of the research dissertation outlines the fundamental concepts governing the working principle of the pulse oximeter device. Here, the research explores some of the different approaches that other researchers have employed in the design and implementation of their model. This research also tried to analyze the grey areas of their approach with the aim of improving on the downsides thereby adding value to the existing body of knowledge on this subject matter. The breakdown of the key concepts involve in the development of pulse oximeter device were also discussed.

2.2.1 Spectroscopy Analysis in Pulse Oximetry

This is the branch of medicine that deals with the biomedical interaction between tissues and electromagnetic radiation as the function of the radiation's wavelength (Cheung *et al.*, 2022). In a more specific term, spectroscopy is the concise study of color ranging from the visible light to other bands of the electromagnetic spectrum. From historical standpoint, it stems from the study of wavelength variation due to absorption by chromophores and gas phase matter of visible light scatter by a prism (Bui *et al.*, 2020). In the field of physics, chemistry and astronomy, it forms a fundamental exploratory tool which helps to pave the way for in-depth intrinsic investigation of the physical structure, composition and electronic structure of matter at the atomic, molecular and macro scale (Elas *et al.*, 2019). It finds very useful application in medicine ranging from biomedical spectroscopy, tissue analysis and medical imaging.

As earlier mentioned, the pulse oximeter is an electronic device whose working principles aims at estimating the level of the peripheral oxygen saturation (SpO_2) of a user non-invasively. In doing this, it tries to approximate the arterial oxygen saturation (SaO_2) which in real sense is defined as the ratio of oxygenated hemoglobin concentration [HbO_2] to the total hemoglobin concentration of the blood [Hb_{total}] under consideration (Tsiakaka *et al.,* 2020). The underlining mathematical formula to illustrate this is in equation (2.1) (Rauniyar *et al.*, 2020)

$$SaO_2 = \frac{[HbO_2]}{[Hb_{total}]} \times 100\% \qquad (2.1)$$

In actuality, the arterial oxygen saturation is what translates to the peripheral oxygen saturation. The term "peripheral" stems from the fact that the oxygen saturation is obtained non-invasively by placing the pulse oximeter sensor at the peripheral parts of the body where there is appreciable blood perfusion. There are two major working principles that is that forms the design of a typical pulse oximeter. These are Photoplethysmography and Spectroscopy.

The pulse oximeter sensor can operate in two major modes, which are Transmittance mode and Reflectance mode.

(1) In the transmittance mode oximeter, the detector is set at the opposite side of the light source such that the investigative tissue becomes in between. This setup is most suitable for placement around the finger or ear lobe.

(2) In the reflectance mode oximeter, the detector is place next to the light source with a demarcation in between such that the measurement relies only on the backscatter of

light. This type is most suitable for placement around the chest or forehead. Figure 2.2 is an illustration of the different modes of operation of the device.

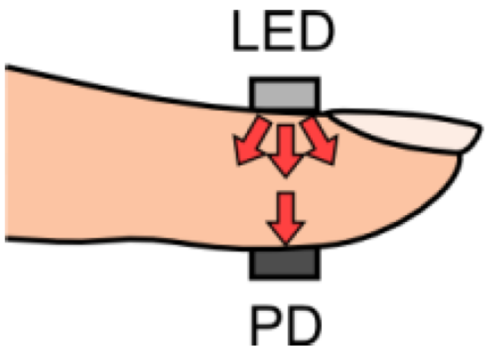

Figure 2.2a: Transmittance Mode Pulse Oximeter Operation (Tamura *et al.*, 2014)

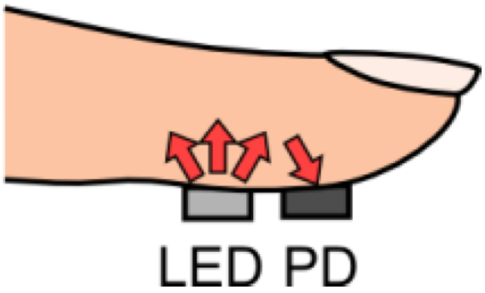

Figure 2.2b: Reflectance Mode Pulse Oximeter Operation (Tamura et al., 2014)

Pulse oximeter is essentially a particular case of the application of optical spectroscopy used to quantify chromophores. Because in the case of the pulse oximeter, the chromophores of primary consideration are the oxygenated and deoxygenated hemoglobin, it requires the use of two distinct radiations of unique wavelengths in order to establish the estimation of the SpO_2. It adopts the use of optoelectronic components like the light emitting diode (LED) to impinge a light flux onto the peripheral part of the body with appreciable blood perfusion (i.e. the photoplethysmographic stage) and then detecting the transmitted (or reflected) light in order to estimate the degree of absorbance of the light by the tissues in the spectroscopic stage.

2.2.2 Saturated Peripheral Oxygen Level

The Saturated Peripheral Oxygen level (SpO_2), is a key measurement parameter in pulse oximetry. The ratio of the absorbance coefficients R of the red and infrared lights in Equation (2.8) and (2.9) enables the calibration of the pulse oximeter device during the course of the design. The SpO_2 value gives an indication of the level of saturated oxygen level in the blood of the user of the pulse oximeter. These includes: the ear lobes, finger, tongue etc. (Tsiakaka *et al.*, 2020). In the event of an outbreak of infectious disease like the novel Covid-19 pandemic, the constant monitoring of the SpO_2 level of the patient can indicate when the condition of the patient is getting to a critical point where the patient may need serious medical attention that can help save the life of the patient under consideration. Many design approach in the measurement of the SpO_2 level of the blood has been developed most of which requires the placement of the pulse oximeter sensor at a suitable part of the body where there is an appreciable amount of blood flow. Figure 2.3 shows the extinction coefficient spectra in oxyhemoglobin and deoxyhemoglobin in the visible and near infrared (NIR) range.

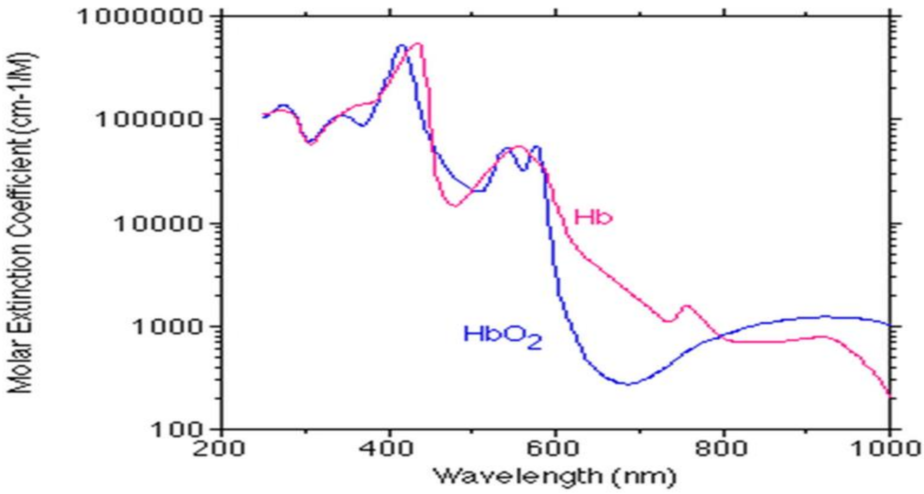

Figure 2.3: Extinction coefficients spectra of oxyhemoglobin and deoxyhemoglobin (Nitzan *et al.*, 2020)

2.2.3 Beer-Lambert's Law

The major law governing the working principle of the pulse oximeter stems from the famous Beer-Lambert's Law (BLL). This law finds application in the quantification of chromophores in a media.

Equation (2.2), (2.3), and (2.4) gives the absorbance $A(\lambda)$ of the light source of wavelength λ (Tsiakaka *et al.*, 2020)

$$A(\lambda) = -\ln\big(T(\lambda)\big) \tag{2.2}$$

$$A(\lambda) = -ln\frac{I(\lambda)}{I_0(\lambda)} \tag{2.3}$$

$$A(\lambda) = \varepsilon_x(\lambda)[X]d(\lambda) \quad (2.4)$$

where:

λ is the wavelength of the illuminating source,

$T(\lambda)$ is the transmittance of the wavelength in the media,

$I_0(\lambda)$ is the intensity of the incident light,

$I(\lambda)$ is the measured output intensity,

$\varepsilon_x(\lambda)$ is the molar extinction coefficient of the chromophore X,

$[X]$ is the chromophore concentration in the media and

$d(\lambda)$ is the optical path length.

The net absorbance by the media containing oxygenated hemoglobin (HbO_2) and deoxygenated (Hb) can then be given by equation (2.5) (Tsiakaka *et al.*, 2020)

$$A(\lambda) = (\varepsilon_{HbO_2}(\lambda)[HbO_2] + \varepsilon_{Hb}(\lambda)[Hb]) \times d(\lambda) \quad (2.5)$$

The absorbance coefficient is usually a product of two major components, which are the AC component and the DC component. The AC component is that part of the signal that emanates due to the pulsatile blood (i.e. those generated from the heart rate modulation). The other larger part is the DC component which is primarily originated from the absorption of light by the surrounding tissues (e.g. dermis, bone, fat, adipose etc.), which is almost constant in time as compared to the AC component.

In order to distinguish between the concentrations of oxyhemoglobin and deoxyhemoglobin, a minimum of light sources of two different wavelengths is required. Thus, the suitable wavelengths chosen for the pulse oximeter design are those of the red light (660nm) and infrared light (940nm). The term pulsatile index is the ratio of the AC component to that of the DC component.

Equations (2.6) and (2.7) (Tsiakaka *et al.*, 2020) gives the perfusion indexes PI(s) of two distinct wavelengths λ_1 and λ_2 for red and infrared light respectively.

$$PI(\lambda_1) = AC(\lambda_1)/DC(\lambda_1) \quad (2.6)$$

$$PI(\lambda_2) = AC(\lambda_2)/DC(\lambda_2) \quad (2.7)$$

where:

$PI(\lambda_1)$ is the pulsatile index for the red light wavelength,

$PI(\lambda_2)$ is the pulsatile index for the infrared light wavelength,

$AC(\lambda_1)$ is the AC absorbance for the red light wavelength,

$AC(\lambda_2)$ is the AC absorbance for the infrared light wavelength,

$DC(\lambda_1)$ is the DC absorbance for the red light wavelength,

$DC(\lambda_2)$ is the DC absorbance for the infrared light wavelength.

Then, the time dependent ratio of the pulsatile index $R(t)$ is given by equation (2.8) (Tsiakaka et al., 2020)

$$R(t) = \frac{AC(\lambda_1)/DC(\lambda_1)}{AC(\lambda_2)/DC(\lambda_2)} \quad (2.8)$$

The ratio of the pulsatile index in terms of the concentrations of the oxygenated and deoxygenated haemoglobin is in equation (2.9) (Tsiakaka *et al*., 2020)

$$R(t) = \frac{(\varepsilon_{HbO_2}(\lambda_1)[HbO_2]+\varepsilon_{Hb}(\lambda_1)[Hb])\times d(\lambda_1)}{(\varepsilon_{HbO_2}(\lambda_2)[HbO_2]+\varepsilon_{Hb}(\lambda_2)[Hb])\times d(\lambda_2)} \quad (2.9)$$

Equation (2.10) (Tsiakaka et al., 2020) gives the time dependent Saturated Peripheral Oxygen $SpO_2(t)$ level.

$$SpO_2(t) = \frac{\varepsilon_{Hb}(\lambda_1)-\varepsilon_{Hb}(\lambda_2)R(t)}{\varepsilon_{Hb}(\lambda_1)-\varepsilon_{HbO_2}(\lambda_1)+[\varepsilon_{HbO_2}(\lambda_2)-\varepsilon_{Hb}(\lambda_2)]R(t)} \quad (2.10)$$

2.2.4 Heart Beat Rate

This is another very important measurement parameter used in the design of pulse oximeter. This parameter gives a measure of the heartbeat of the user per minute. The successive peaks or troughs of the bionic signal per time, gives a measure of this parameter. Here, the acceptable range of values for a healthy adult ranges from 60 to 100 beats per minute (bpm) (Chacon *et al.*, 2018). A value outside this range is indicative of an abnormal health condition that requires an appropriate medical attention. In a nonprofessional's language, the pulse rate is the estimation of the number of times that the human heart contracts per minute. In a more generic term, a lower heart rate could imply more efficient heart function and better cardiovascular activity. For some individuals, a pulse rate below 60 bpm indicates an abnormally slow heart action, which is also known as bradycardia (Buckley & Salpeter, 2015). In actuality, the pulse oximeter device can offer the user the ability to get an accurate insight of the user's SpO_2 and pulse rate within a matter of few seconds so that prompt actions can be taken in the event of abnormal reading. Figure 2.4 shows the heartbeat per minute as a function of time for different parts of the body where there is appreciable blood perfusion during rest, light exercise, and moderate exercise.

2.2.5 Critical Threshold Assignment Triage

This refers to the assignment of degrees of urgency to wounds or illnesses with the aim of determining the order of treatment of a large number of patients or casualties (Kalid *et al.*, 2018). In situation where it becomes very important to be able to assess the degree of severity of the health conditions of patients in order of precedence, the pulse oximeter will be a handy solution to such a problem. Therefore, the designed pulse oximeter modules should have the ability to relay the measured data to a central repository wirelessly without having any close contact with them. This is what informed the incorporation of the Bluetooth wireless module for wireless communication with a PC terminal.

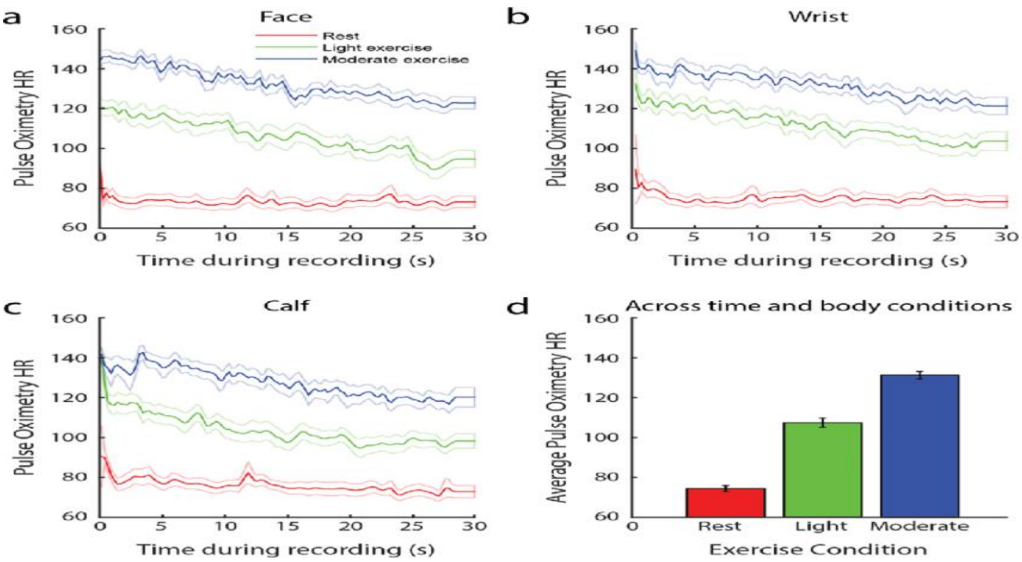

Figure 2.4: Pulse Oximetry Based Heart Rates in Beats per Minute Referenced as a Function of Time (van der Kooij & Naber, 2019)

Table 2.1 gives the range of values of measurement parameter, as yardstick to determine the degree of the severity of a patients' health condition in the event of an outbreak.

Table 2.1: Normal Range of Values of Oxygen Saturation, Heart Beat and Temperature in the Human Body (Utomo *et al.*, 2019)

Test Metric	**Normal Range of Values**	**Abnormal Normal**
Oxygen Saturation	95-100 %	Below 90 %
Heart Beat	60-100 BPM	below 60 BPM
Temperature	36^0C-37.2^0C	< 36°C and >38°C

The medical practitioners observe it from Table 2.1 that values outside the normal range is indicative of an abnormal state of health of the patient and as such, will require the appropriate medical attention.

2.2.6 Short Range Wireless Technologies

Bhalla and Bhalla, (2010) defined wireless technology as the transfer of information over a spatial space without the use of electrical wires. The distance in which this information is transferred can be a short or long one depending on the application or specification of the communication architecture. For this research work, the application of short range wireless communication is where more emphasis will be placed. This is because the type of wireless communication that was adopted in the course of this research falls under this category. The evolution of health care systems into the digital domain has made the need for short range wireless technologies in health care data exchange applications a more sort after enterprise in recent times (Vidakis *et al.*, 2020). Some of these technologies will be discussed in the ensuing subsections.

2.2.6.1 ZigBee Wireless Communication

This technology is among the list of high-level communication protocols. It is an IEEE 802.15.4-based communication protocol specification. It is a low power, low data rate and close proximity wireless technology which can be used to establish a Personal Area Network (PAN) with different types of wireless radios technologies that finds application in home automation and medical device data collection. ZigBee is use in small-scale hobbyist projects that requires the use of wireless connectivity. This is a cheaper and simpler wireless technology than other conventional ones like the Bluetooth or Wi-Fi applications. By operational principle, this wireless technology operates within the universal unlicensed frequency band of 2.4 to 2.4835 GHz with sixteen channels slots that are spaced by a 2MHz band. The wireless radios involve in this type of technology use a direct sequence spread spectrum coding where a digital stream manages the flow of data into the modulator. In the 2.4GHz universal band application of this technology, an Orthogonal Quadrature Phase Shift Keying (OQPSK) that transmit two bits per symbol is used. The raw data rate of this technology is 250kbits/s per channel; the average transmission range is around 10-20m, which largely depends on the construction materials while the output power is generally between 0-20dBm (i.e. 1-100mW).

2.2.6.2 Wi-Fi Communication

The wireless fidelity (Wi-Fi) communication is a very powerful technology that has gained a huge popularity in the past few decades because of its robust and efficient architecture. It has also gained some very important application areas like the internet of things (IoT), smart wireless connectivity etc. It's radius of coverage can go as high as 150ft or 45m and it also harnesses the use of the 2.4GHz free band spectrum for communication. Many shopping malls and cafes in the world use this technology to cater for their wireless network connectivity needs. In most cases, a Wi-Fi network creates a wired network to a router. This network establishes wireless access to other devices. These devices can then connect to the network by providing the appropriate passkey required for access to the wireless network in the case of a secured wireless network. This is often the case with many establishments. Hand-held mobile devices via the use of mobile hotspot can also create it in order to enable wireless communication between the mobile device and other mobile devices or accessories.

2.2.10.3 Bluetooth Wireless Communication

The Bluetooth wireless communication is a short-range wireless communications technology that replaces connection cables used in connecting smaller devices to provide a more robust level of wireless security. This wireless communication is based on what is popularly known as Ad-hoc technology (or Ad-hoc Pico nets), which essentially connotes a type of local area network with a much smaller coverage. It makes use of the 2.4GHz free band of wireless communication amongst smaller gadgets and accessories within a short coverage radius of about 10 meters.

In this research work, the use of Bluetooth wireless communication in order to provide added functionality to the pulse oximeter device that will aid the ease of the monitoring process of the state of health of patients in a medical ward by medical practitioners. Another advantage that we envisage will accrue to the adoption of this technology in our work is the fact that, the use of the Bluetooth wireless communication can help to reduce the risk of exposure of medical practitioners to infectious diseases in the event of an outbreak of a pandemic. In addition to this, the ambulation of patients within the medical ward while carrying out real time medical exam becomes easy.

In this research work, a wireless communication protocol interface was used to implement wireless communication between the personal computer software and the pulse oximeter device as shown in the Figure 2.5.

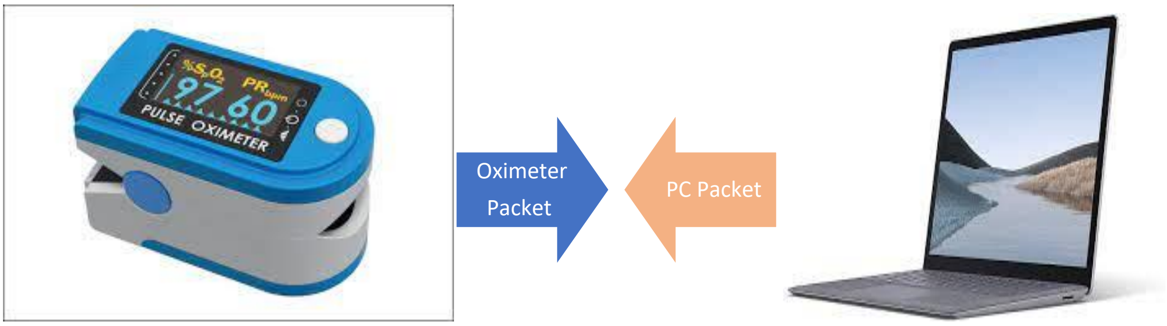

Figure 2.5: Packet exchange between pulse oximeter and PC via the wireless Bluetooth channel

Figure 2.6 and 2.7 shows an illustration of the data packet scheme sent by the pulse oximeter and a Personal Computer (PC) during data communication.

Section	Header				Body	Tail
Sub-Section	Preamble	PC-Address	Oximeter Address	Command	Data Payload	Terminator
Data-Width	2Bytes	4Bytes	4Bytes	2Bytes	1-32Bytes	2Bytes

Figure 2.6: Format of Data Packet Sent by Pulse Oximeter

Section	Header				Body	Tail
Sub-Section	Preamble	Oximeter Address	PC-Address	Command	Data Payload	Terminator
Data-Width	2Bytes	4Bytes	4Bytes	2Bytes	1-32Bytes	2Bytes

Figure 2.7: Format of Data Packet Sent by Personal Computer

The formula for calculating the root mean square error of the measurements between two quantities is expressed in Equation (2.11)

$$RMSE = \sqrt{\frac{\sum(X_1 - Y_1)^2}{N}} \tag{2.11}$$

where:

RMSE is the root mean square error,

N is the number of sample, and

$\sum(X_1 - Y_1)^2$ is the summation of all the square errors.

SECTION THREE
MATERIALS AND METHOD

3.1 Introduction

This chapter gives a detailed breakdown of the systematic procedures and methods used to realize the implementation of the research. Section 3.2 gives a list of the materials used to achieve the individual functional blocks of the research while section 3.3 elucidates on the methodology adopted in the improvement of the performance of the system thus far.

3.2 Materials Used

The list of the materials used for the implementation of this research work is listed below:

1. 16 by 2 green LCD display
2. PIC16f887 Microcontroller unit
3. LM7805 +5V voltage regulator
4. M29150 +3.3V voltage regulator
5. ZigBee wireless module
6. Max30100 Oximeter Sensor module
7. Level shifter module
8. C1815 transistors
9. Diodes
10. Soldering Iron
11. Soldering Led
12. Led sucker
13. Jumper wires
14. Arduino Serial Plotter terminal
15. Buzzer
16. LDR

17. Small red-LED
18. 12V DC adapter socket
19. Push buttons
20. Yellow plastic push button caps
21. 9V battery
22. 9V battery socket
23. Crystal Oscillator
24. Capacitor
25. Perspect plastic casing
26. Resistors
27. IC sockets
28. Male and female socket header
29. Pickit 3 Programmer
30. Proteus Circuit Development suite
31. Proton Compiler Software
32. Matlab

3.3 Methodology

The methodology that was used to carry out this research work is broken down as follows:

1. Development of an adaptive algorithm to mitigate the effect of varying ambient light and temperature through the following steps:
    a) Measurement of the ambient light and temperature of the surrounding.
    b) Computation of the compensation factor μ.
    c) Recalculation of the wavelength ratio R_{μ}.
    d) Recalculation of the improved SpO_2 value.

2. Development of a locally made prototype based on the work of (Metcalfe *et al*., 2021) and improvement of the overall performance through the incorporation of the algorithm developed in methodology 1. This was achieved through the following steps:
    a) Implementation of the hardware subcomponents using a breadboard for preliminary test before transferring to a Vero-board.
    b) Implementation of the firmware using visual abstraction framework as encapsulated in the state transition diagram on Figure 3.17.
    c) Programming of the hardware component using the visual abstraction framework in b) with the visual basic programming language.
    d) Incorporation of a wireless communication interface using a Bluetooth wireless module and an established wireless communication protocol shown on Figure 2.12 and 2.13.
3. Evaluation of the performance of the developed algorithm through the following steps:
    a) Measurement of SpO_2 and heart rate values with the design model and an existing clinical model.
    b) Repeating the process in step a) under varying ambient conditions to obtain the resultant SpO_2 and heart rate values.
    c) To calculate the Root mean square error for both the SpO_2 and Heart rate values obtained in steps a) and b) and ascertain whether the computed value is within the acceptable limits.

3.3.1 Design and Development of Locally Made Prototype

Under this section, detail breakdown of the hardware design alongside with the circuit schematic explaining the design procedure adopted in achieving the desired functionality of the functional unit forms the epicenter of this subsection. The subdivision of the hardware design was examined under the ensuing subsections in a bid to give a detail description of how the whole process was achieved during the course of the conduct of the research. These explanations goes as follows:

3.3.1.1 Hardware Implementation

This subsection talks about the details of the hardware design conceived in developing the locally made prototype. Here, each functional unit was taken and explained further for the purpose of clarity and understanding as follows:

(1) Power Supply Section

In order to achieve the successful implementation of this research work, two major DC voltages of interested was needed which are 5V and 3.3V. These voltage specifications is a consequence of the provisions made in the datasheets of the microcontroller unit and the accompanying peripheral components.

The PIC16f887 microcontroller, the LCD display and the buzzer units requires the use of 5V nominal voltage for their correct operation while the Max30100 and the Bluetooth wireless module requires the use of 3.3V for their normal operation. In order to obtain these voltages, two different IC voltage regulators were used. The LM7805 was used to provide the +5V regulation and MIC29150 for the 3.3V regulation (Hsu *et al.*, 2013). By design specification, the LM7805 IC regulator requires the use of a nominal input DC voltage range of 7V to 15V (Rizman *et al.*, 2013).

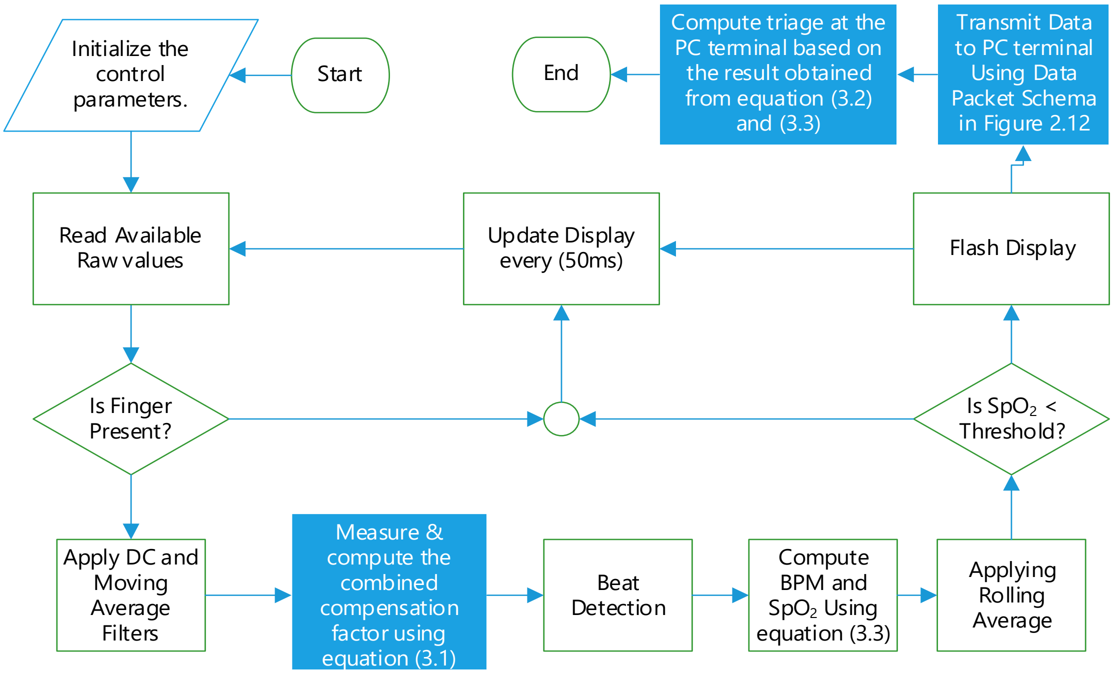

Figure 3.1: Flowchart of the Improved Model

Figure 3.2 illustrates the schematic diagram for the power supply design adopted for the research work.

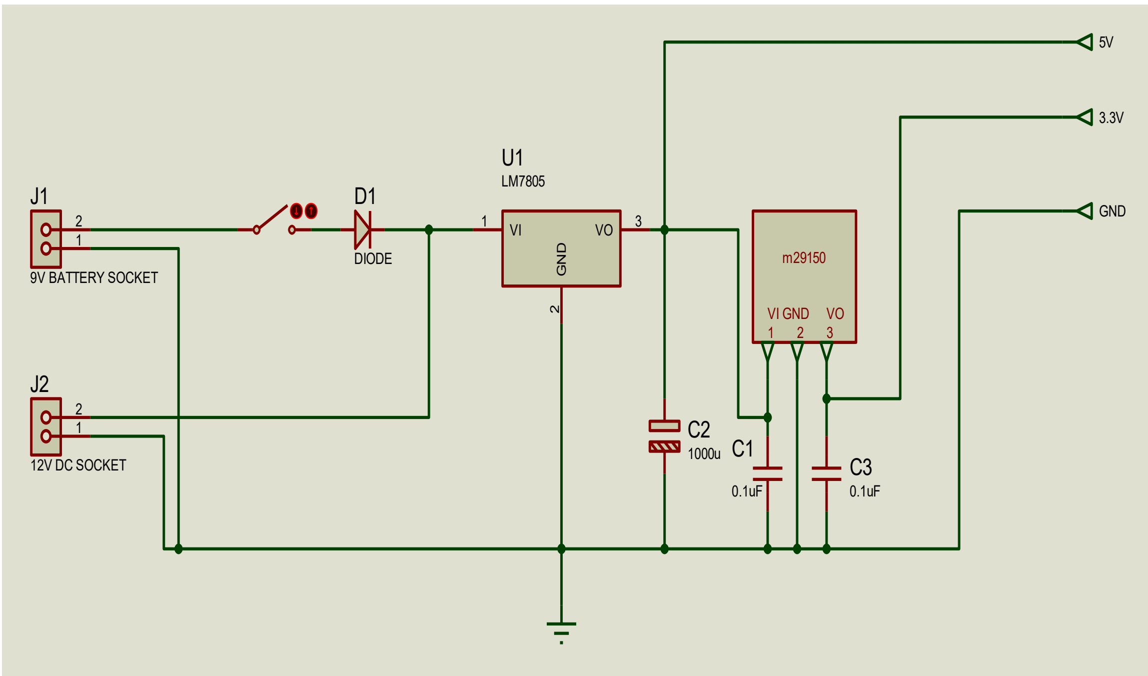

Figure 3.2: Schematic Diagram of Power Supply Design

As it can be seen, the power supply design consists of two voltage regulators; the M29150 is fed by the voltage output of the 5V regulator. The MIC29150 takes an input voltage of 5V and produces an output voltage of 3.3V. Thus, the LM7805 produces the output voltage of 5V while the MIC29150 is used to produce the output voltage of 3.3V (Current *et al.*, 2012). On the other hand, the input to the LM7805 is fed by two DC sources, J1 and J2 for 9V battery and 12V adapter sockets respectively. The battery supply is fitted with a make and break switch alongside a reverse biased blocking diode to impede reverse charging current that may flow from the 12V DC supply to the battery as this can lead to overcharging of the battery and consequently leading to explosion or fire outbreak. The output of the LM7805 is further filtered by a 1000uF bulk filtering capacitor and a 0.1uF high frequency noise filter. The output of the 3.3V regulator is also filtered with a 0.1uF capacitor for high frequency ripples.

(2) Liquid Crystal Display Section

This is the section of the research design that provides the primary output for users. Under this design, two key parameters form the major focus of the design. This includes:

(a) The LCD contrast and

(b) The LCD brightness.

In manual contrast adjustment design, it is recommended that a variable current sinking resistor of 10kΩ-20kΩ between the contrast pin of the LCD and ground be used as it is in the Figure 3.3.

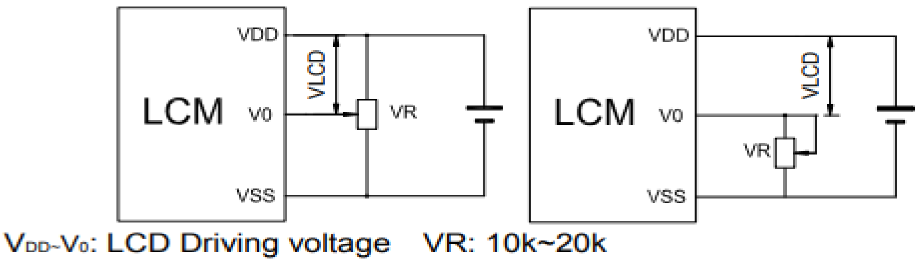

Figure 3.3: Contrast Adjustment Setup of a 16 by 2 LCD Screen (Cameron, 2019)

With such a setup, the contrast setting can only be adjusted manually through the use of the variable resistor knob. But in the design approach adopted for this research, the contrast adjustment is desired to be implemented via firmware and as such, a transistor connected in a common emitter configuration was used to connect the contrast pin to ground. Hence the contrast of the display can be varied by software through the use of the digital to analog (DAC) pin PORTC.2 of the PIC16f887 microcontroller (İnce, 2020), whose output voltage is applied to the base of the transistor through a current limiting resistor as shown on Figure 3.4. Figure 3.5 is a schematic diagram of the buzzer circuit.

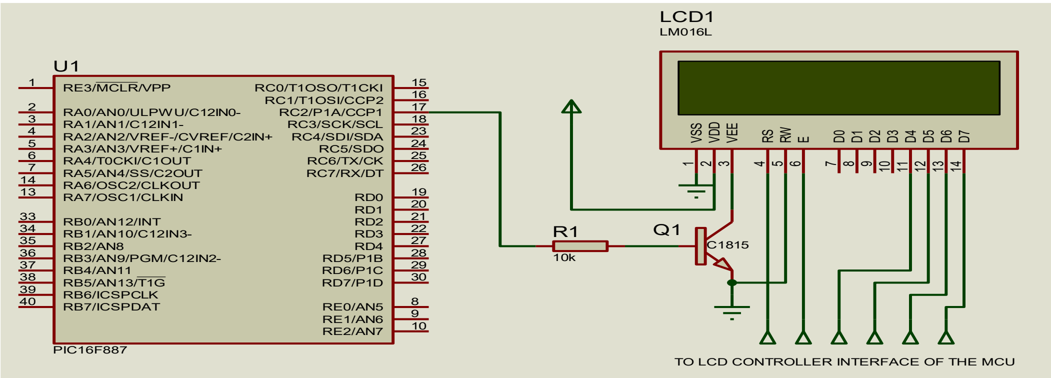

Figure 3.4: Hardware Design of a Software Adjustable Contrast Setting from an MCU

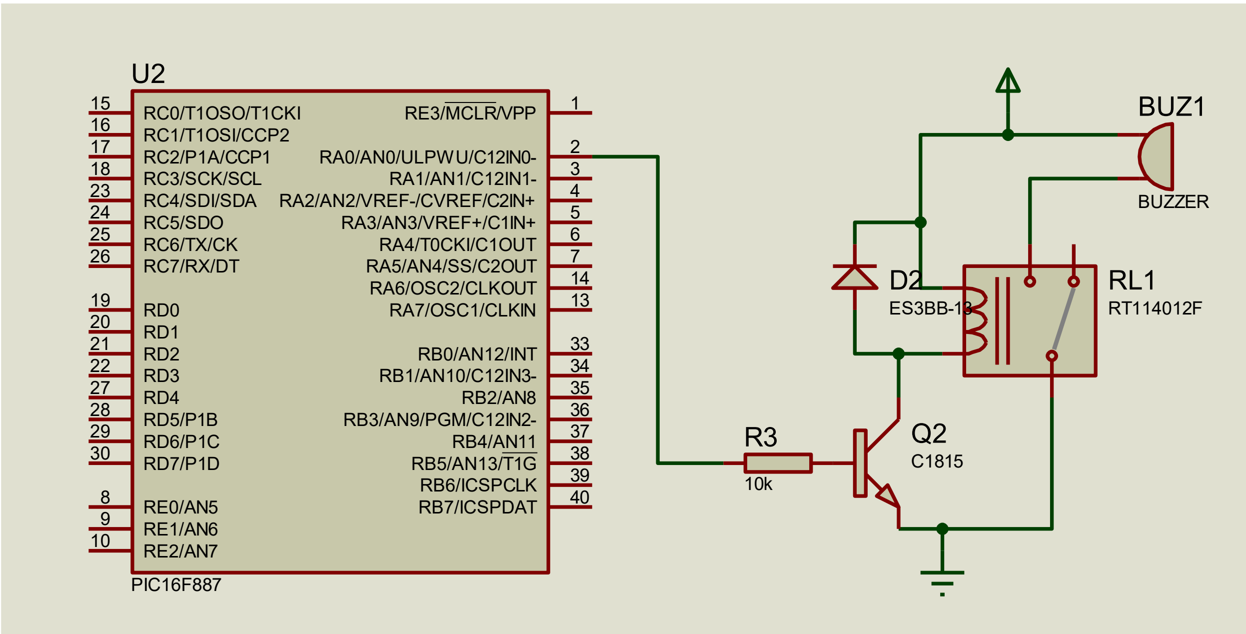

Figure 3.5: Schematic Diagram of the Buzzer Circuit

The block diagram of the max30100 oximeter sensor shown on Figure 3.6, consists of the red and infra-red LEDs the photo-detector, the LED drivers block, the oscillator block, the digital filter, the data register block, the ambient light cancellation block and the I2C communication engine block. All these blocks of functional units work together in synchrony in order to generate the desired photoplethysmographic signal needed for the determination of the peripheral oxygen saturation (SpO_2) and the heart rate.

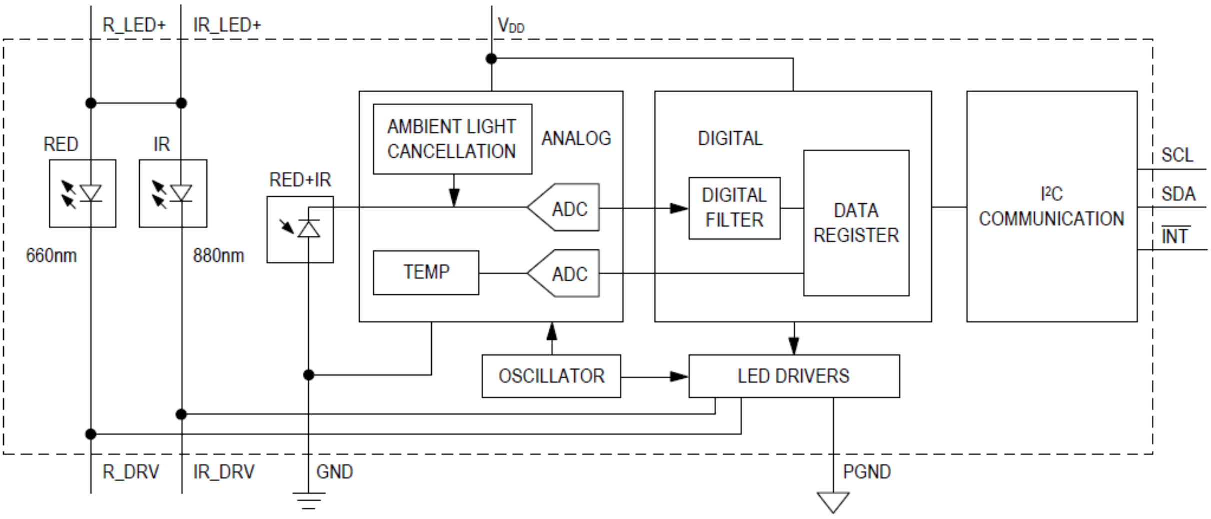

Figure 3.6: Block Diagram of Max30100 (Pham *et al.*, 2020)

The max30100 oximeter sensor module is designed to operate with 3.3V while the PIC16F887 microcontroller IC that was used for the research is designed to operate with a voltage of 5V. The discrepancies in the operational voltages of the MCU and the Max30100 makes it necessary to employ the use of the voltage level shifter module to connect the signal control pins of the microcontroller and that of the max30100. Figure 3.7 shows the schematic diagram of the connection between the microcontroller and the max30100.

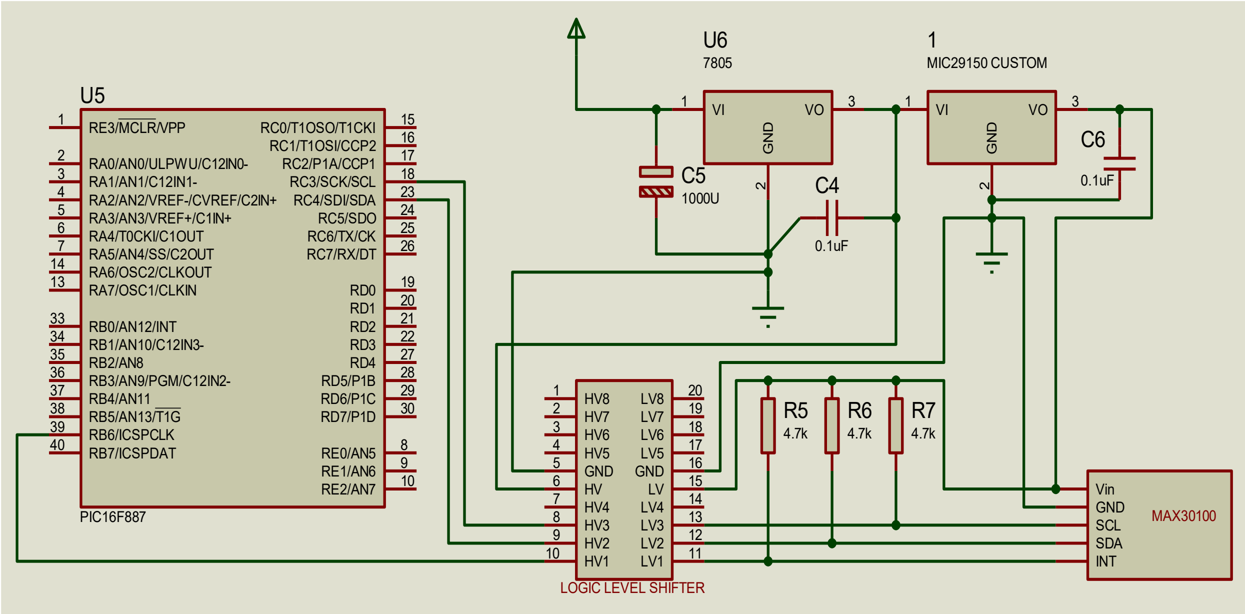

Figure 3.7: Schematic Diagram of the Max30100 Oximeter Sensor Interface

(3) Determination of Heart Rate

In the design approach adopted for this research work, frantic effort was made towards minimizing the computation time required to determine the heart rate by the designed model. In order to determine the heart rate, the major task involves calculating the average period between the sampled pulsations obtained from the oximeter sensor. This value is consequently indicative of the rate of cardiac activity, and used to calculate the heart rate through a mathematical relationship that exists between frequency and period of a signal. Through the changing volumetric flow of venous blood that result in a pulsating bionic signal detected by the pulse oximeter sensor, a photoplethysmographic plot of the pulsatile component of the blood is formed. In order to achieve this feat, the timer1 module of the PIC16f887 as the time base for obtaining the period of the pulsation. In the design that was adopted for this research, the timer1 module was configured to operate with the internal frequency execution cycle clock (FOSC/4), which is in real sense a division by a factor of four of the crystal oscillator frequency driving the microcontroller. The computational overhead involved in the max30100 subroutine, necessitated the use of a crystal oscillator of 20MHz. In order to minimize the frequency of the calls to the timer1 subroutine (which occurs whenever the two-byte timer1 register overflows), the highest timer1 prescaler configuration value of 1:8 was selected. Hence, the incremental frequency of the timer1 register can then be calculated using Equation (3.17). The inverse of Equation (3.17) gives the incremental period of the timer1 register using the chosen configuration which is captured in Equation (3.18) while the total period of a single pulse is given by equation 3.40.

$$F_{inc} = (F_{int}) \times PS \quad (3.1)$$

where:

F_{inc} is the timer1 register incremental frequency,

F_{int} is the internal instruction execution cycle clock,

PS is the selected prescaler value.

The pulse period is then given by Equation (3.18).

$$T_p = \frac{65536 \times N_{RC} + TMR1}{F_{inc}} \quad (3.2)$$

Where:

T_p is the pulse period for one heart-beat,

N_{RC} is the number of timer1 overflow interrupt routine calls, and

$TMR1$ is the timer1 register value.

The pulse rate frequency is the inverse of the pulse incremental period and is given by Equation (3.19).

$$F_p = \frac{F_{inc}}{65536 \times N_{RC} + TMR1} \quad (3.3)$$

Equation (3.19) was used to obtain the number of pulse samples in one second. The average of three of these values is calculated from three consecutive pulses in order to obtain the average pulse as given in Equation (3.3).

frequency F_{pave} given in equation (3.4).

$$F_{pave} = \frac{F_{p1}+F_{p2}+F_{p3}}{3} \quad (3.4)$$

where:

$Abs(F_{p1} - F_{p2}) < t_{min}$, and $Abs(F_{p2} - F_{p3}) < t_{min}$

F_{pave} is the average pulse frequency,

F_{p1}, F_{p2}, and F_{p3} are the three consecutive pulse frequencies,

$Abs(\,)$ is the positive/absolute value of argument inside the parenthesis, and

t_{min} is the minimum tolerance.

The heart-rate is then computed using the formula in equation (3.5). Thus:

$$HR = 60 \times F_{pave} \quad (3.5)$$

3.3.2.2 Software Design Section

The brain behind the intelligence of the device is the microcontroller unit (MCU) and this intelligence is enshrined in a component called firmware which is essentially the software program that runs on the microcontroller. The process of transferring this intelligence to the microcontroller is what is known as embedded system programming. This section is designed to give a breakdown of the software component of the overall design. Because of the myriads of peripheral accessories available in the design such as the LCD display, LED indicator, buzzer and other functionalities of the design, the software design was broken down into MENU like structure so as to enable the user access the various functions of the pulse oximeter design. Figure 3.8 gives the breakdown of the algorithm used for the menu structure of the software design. As it can be seen from the aforementioned Figure, the algorithm of the firmware design gives a panoramic framework of the overall programming approach used for the design of the pulse oximeter which was adopted for this research. As it can be observed, the ovals marked A, B, C, D, E, and F are linkers used to connect the different sectional breaks in the algorithm. Hence two ovals marked with the same letters are said to be connected. From the start of the algorithm, inclusion of libraries, declaration and initialization of control variables follows next. After the initialization of control variables, the programs execution goes to the off-state loop waiting for the press of the power button for up to three seconds. When this is done, the device is switched ON for use and immediately goes to the

ON-state loop where other functions of the Device can be accessed starting from the default menu. The default menu is primarily the place where the oximeter measurements can be carried out and displayed accordingly. From the default menu, if the enter button is pressed; the device goes to the menu options where the settings and adjustments of the peripheral components and access to other functionalities of the design can be obtained. If however the user decides to press the power button for up to 3 seconds from the default menu, the device will be switched off and the program execution will be redirected back to the off loop. From the menu options, the user can browse through the myriads of available features of the pulse oximeter design. These features are further explained in the transition state diagram of the menu options given on Figure 3.9.

When the enter button is pressed while in the menu option, the program execution is send to the first option of the children elements of the parent option that was selected. After reaching the lowest option from a tree branch, the program execution is automatically sent back to the default menu where it can continue with the pulse oximeter measurement based on the current settings that have being effected from the menu options prior to the press of the enter button. Notice also that the press of an exit button while in the menu option causes the program execution to go to the parent option up the hierarchy. Based on the approach used, the individual options that can be accessed in the pulse oximeter, is determined by the value of the command (CMD) which was declared as a byte variable. The action that will be performed when any of the device buttons is pressed is dependent on the previous value of CMD prior to the press of the button.

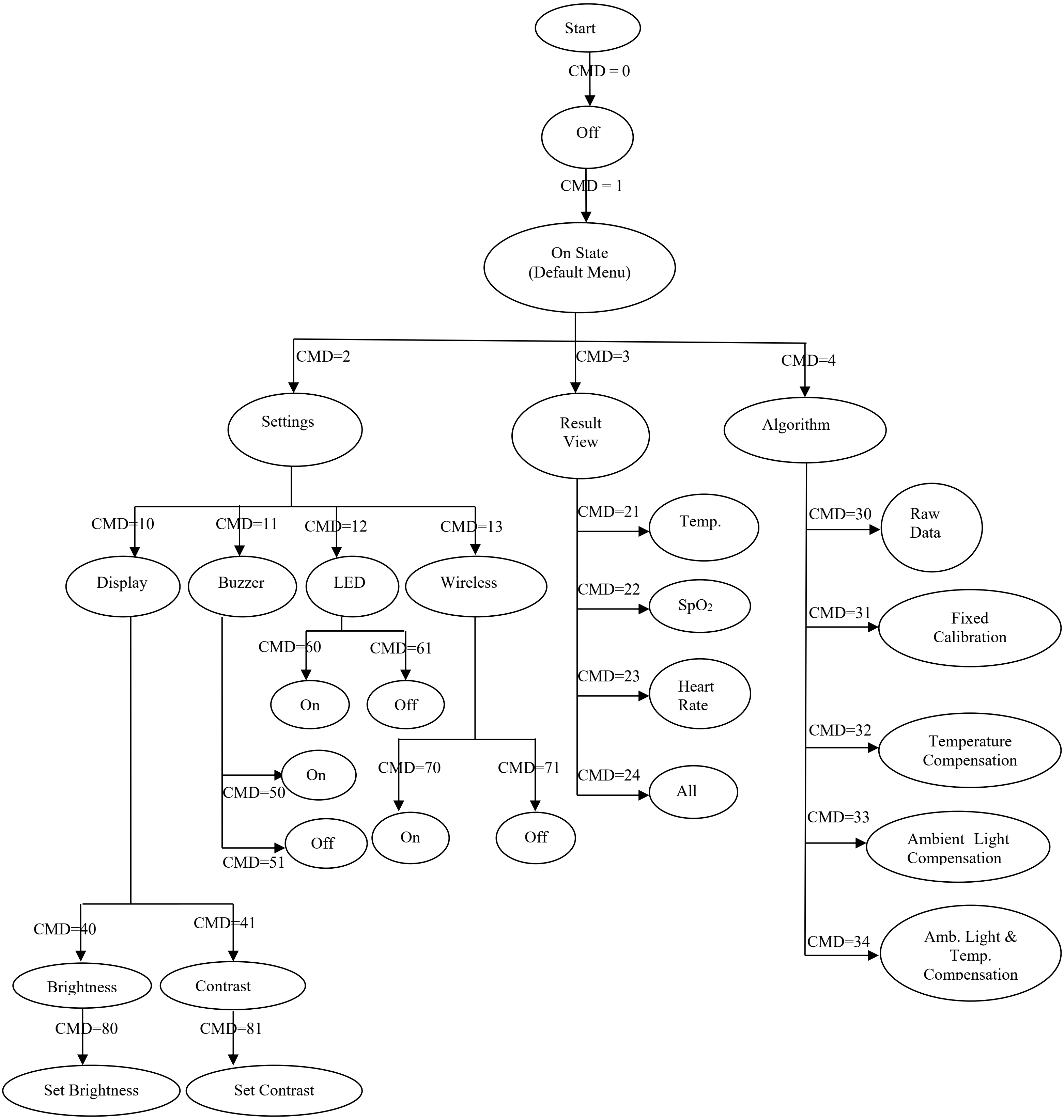

Figure 3.10: State Transition Diagram for the MENU architecture of the Pulse Oximeter Design

SECTION FOUR

PROJECT BUDGET, FEASIBILITY STUDY REPORT, BUSINESS PLAN AND PROJECT TEAM

The following is the commercialization cost estimate for the Development of a Microcontroller-based wireless pulse oximeter for COVID-19 Detection and beyond

Table 1: Cost Breakdown for Commercialization Purpose

Category/Type	**Description**	**Estimated Cost (₦)**	Purpose/Justification
1. Engineering Product design	**a**. Final hardware redesign. **b**. Mass-prototype refinement. **c**. Finished Industrial casing. **d**. Firmware enhancement/optimization	**a.** 1,000,000 **b.** 3,900,000 **c.** 900,000 **d.** 700,000	**a.** To ensure medical accuracy. **b.** To upgrade prototype to production-grade version. **c.** To ensure durability and medical accuracy
2. Assembly and Production set-up	**a**. Purchasing of tools for assembly purpose. **b**. Putting together soldering/rework stations **c**. Leasing of SMT machine quality control tools	**a.** 4,500,000 **b.** 1,500,000 **c.** 2,000,000	**a.** To enhance the setup of small-scale assembly line for over 1,000 devices.
3.Procurement of components and materials	**a**. Order and Purchasing of Sensors (MAX30100/alternative) **b**. Mass purchase of microcontrollers **c.** Order and purchase of Zigbee/Wi-Fi modules **d.** Purchase of PCBs, batteries, casings	**a.** 4,500,000 **b.** 2,500,000 **c.** 1,400,000 **d.** 1,600,000	**a.** To carry out bulk purchase for pilot production of over 1,000 to 1,500 units.
4. Certification, calibration and testing process	**a.** Standard Organization of Nigeria (SON) quality certification. **b.** NAFDAC Registration **c.** Clinical validation trials	**a.** 500,000 **b.** 900,000 **c.** 600,000	**a.** To ensure the process of carrying out market authorization.

			b. To enable compliance with international health standards
5. Integration of cloud and software	**a.** Securing cloud storage **b.** Build up of data analytics dashboard. **c.** Development of patient monitoring app.	**a.** 2,500,000 **b.** 3,000,000 **c.** 1,000,000	**a.** To ensure/optimize data visualization **b.** To enable remote health monitoring. **c.** To ensure a scalable IoT future.
6. Branding and Packaging	**a.** Designing of prototype **b.** High standard Labeling **c.** Designing and duplication of instruction manuals **d.** Production of Packaging materials	**a.** 500,000 **b**. 200,000 **c.** 500,000 **d**. 300,000	**a**. To carry out standardization **b**. To carry out branding that is appealing to the consumer.
7. Marketing & Publicity	a. For Product launching event. b. For carrying out promotional videos. c. For social media activities and medical exposition	**a.** 1,000,000 **b.** 1,000,000 **c**. 1,000,000	**a.** To carry out Awareness campaigns. **b.** To carry out follow-up/adoption campaign that targets hospitals, clinics, and NGOs
8. Product **Distribution** and **Logistics** process	a. For transportation purposes b. For warehousing of products. c. Distribution of products to health facilities nationwide	a. 500,000 b. 1,500,000 c. 500,000	a. To ensures a flexible process of product availability across target regions all over Nigeria.
9. Personnel awareness seminars and **Training**	a. This include technical staff. b. This include engineers of all practices c. This include administrative team heads and members training of sales agents all over Nigeria.	a. 1,500,000 b. 1,000,000 c. 1,500,000	a. To ensure 6–9 months of deliberate staffing and capacity building in preparation for the commercialization phase of the project.

10. Legality and intellectual proprietorship	a. For the purpose of patent filing b. For carrying out trademark registration c. For carrying out legal consultancy	**a.** 500,000 **b.** 200,000 **c**. 300,000	**a.** To ensure the protection of intellectual property **b.** To ensure proper legal compliance
11. Maintenance action of products and **Support Infrastructure** buildup	a. For carrying out customer service setup b. For getting after-sales technical product support tools c. For getting spare parts/Components	**a.** 500,000 **b**. 500,000 **c.** 500,000	a. To ensure b. To ensure product reliability c. Planning for post-deployment maintenance
12. Planning for **contingenc**ies / **Risk Management** planning	a. Making 5% reservation plan for inflation b. Planning for possible component price fluctuation. c. Planning for unforeseen expenses as regards the product	a. 1,000,000 b. 1,450,000 c. 1,500,000	a. Carrying out financial cushion against project risks and the likes.
TOTAL ESTIMATED COST		**₦49,950,000**	

THE FEASIBILITY STUDY REPORT

The Feasibility Study Report for this project is given in table 2.

Project Title: Development and Commercialization of a ZigBee-Enabled, Microcontroller-Based Pulse Oximeter with Machine Learning-Based Hypoxemia Detection

Table 2: Projects Feasibility Study Report

Section	**Description**
1. Project Overview	This project aims to design and commercialized a low cost, ZigBee-enabled pulse oximeter integrated with a random forest-based ML algorithm for real time SpO_2 and pulse-rate monitoring. It focuses towards hospitals, clinics, and home healthcare in Nigeria.
2. Project Objectives	1. Design and implementation of a wireless, microcontroller-based oximeter. 2. Development of adaptive machine learning for accurate hypoxemia detection. 3. To validate and compared the performance of the design system using MAE and RMSE as the benchmarks.
3. Project Market Need	The high demand for affordable and accurate medical devices in Nigeria, currently dependence on costly importation. Hence, increasing awareness of respiratory health post covid-19, grows telemedicine and home care markets.
4. Project Technical Feasibility	Based on well know technology, Such as Arduino compatible microcontrollers, MAX30100/30102 sensors for SpO_2 measurement, ZigBee is use for wireless data transfer, and ML algorithm written in python embedded C. The components are readily available and locally assembly is possible.
5. Project Economic Feasibility	The estimated initial production cost per unit is ₦20,000 to ₦25,000, ₦40,000 to ₦50,000 is the selling price. Gross margin estimate is 45 to 55%.30 to 50 technical and assembly jobs positions could be created within the next first years. Payback time is about 2 years.
6. Project Financial Requirements	The anticipated total commercialization cost estimated is ₦50 million. This comprises marketing and distribution certification (NAFDAC/SON), production setup and R&D optimization. Grant money and possible private co-investment.

7. Project Regulatory Feasibility	This requires SON certification for quality and safety as well as NAFDAC registration (medical device category). The plans are in place to Comply with ISO 13485 and IEC 60601 standards.
8. Project Operational Feasibility	The production can take place in a university technological hub or an existing electronics fabrication factory. For testing, calibration and assembly local technicians received training. Collaboration for pilot testing with hospitals.
9. Project Environmental Feasibility	Combing low power components and rechargeable batteries, making it environmentally safe. Plans for recycling used sensors and components, minimize electronic waste.
10. Project Social Feasibility	Enhancing access to healthcare in rural and underprivileged areas, supporting government's goal for improving digital health infrastructure and job creation. Increasing public trust in domestically produced medical devices.
11. Project Risk Analysis	Technical fluctuation in sensor accuracy, market and importation competition; Regulatory: delays in certification; Financial: changes in component prices. Mitigation strategies include modular design for upgrades, early certification engagement, and local sourcing.
12. Project Expected Benefits	Data-driven from medical decisions, better healthcare delivery and lower mortality from respiratory diseases, job development, import substitution, and more foreign exchange retention through domestic manufacture.
13. Project Implementation Timeline	**12 months** 1. Months 1 to 2 is design and optimization 2. Validation of prototype from months 3 to 4 3. Production setup and certification start from months 5 to 2 4 During months 9 to 12, test marketing and distribution
14. Project Conclusion	This project is achievable from a technical, financial and social standpoint. The oximeter has the potential to revolutionize Nigeria's domestic medical device industry, improve healthcare efficiency, and spur economic growth in the country with the right finance, regulatory compliance, and industrial partnership.

FRAMEWORK OF BUSINESS PLAN

PROJECT MANAGEMENT TEAM

Personnel	Name	Contact Information
Principal Investigator (PI)	Dr. Idris Musa	im4idrismusa@yahooco.uk +234(0)8145512666
Co-PI	Prof. A. D. Usman	aliyuusman1@gmail.com 08066238363
Research Assistant 1	Dr. Agbon E. E	eagbonehime1@gmail.com 07061636968
Research Assistant 2	Dr. A.S. Yaro	asyaro@gmail.com 08069254680
Project Manager Head	Dr. H. Bello	bellohabeebu@yahoo.com 07036667227
Software Development Analyst	Monday Francis	mondayfrancis@gmail.com 07065887667
Head of Finance, Marketing and Commercialization	Athanisius Terlumun Utev	utevterlumun@gmail.com 08028213292

CONCLUSION

The development and commercialization of more robust medical equipment has become an imperative in this modern era. However, many technical overheads abound that tries to limit the extent that this can be done. This therefore necessitates the need for more frantic efforts to be made in the development of mathematical models, algorithms and error minimizing hardware peripherals that will be very pertinent in the realization of more robust designs. In this research, one of the major causes of error imposition to the bionic signal was observed to be that of ambient light temperature and motion artifacts which was largely mitigated by the use of a novel fixed window algorithm, ambient light and temperature compensation algorithms. The fixed window algorithm allows for the dynamic tracking of the maxima and minima points of the bionic signal regardless of the imposition of noise by motion artifact thus improving the accuracy of the result obtained by the pulse oximeter. On the other hand, the ambient light and temperature compensation algorithms, enabled the designed system to adapt to marked changes in the ambient light and temperature conditions of the place wherein the device is deployed for use. All these algorithms put together made the overall performance of the designed model better than that of the base paper. The performance index that was used to establish the performance improvement was that of the root mean square error for the SpO_2 and Pulse Rate.

REFERENCES

Bhalla, M. R., & Bhalla, A. V. (2010). Generations of mobile wireless technology: A survey. *International Journal of Computer Applications, 5*(4), 26-32.

Buckley, J. S., & Salpeter, S. R. (2015). A risk-benefit assessment of dementia medications: systematic review of the evidence. *Drugs & aging, 32*(6), 453-467.

Bui, N., Nguyen, A*., et al.* (2020). Smartphone-based spo2 measurement by exploiting wavelengths separation and chromophore compensation. *ACM Transactions on Sensor Networks (TOSN), 16*(1), 1-30.

Cesari, M., & Proietti, M. (2020). COVID-19 in Italy: ageism and decision making in a pandemic. *Journal of the American Medical Directors Association, 21*(5), 576.

Chacon, P. J., Pu, L*., et al.* (2018). A wearable pulse oximeter with wireless communication and motion artifact tailoring for continuous use. *IEEE Transactions on Biomedical Engineering, 66*(6), 1505-1513.

Chen, C., Zhang, X., Ju, Z., & He, W. (2020). Advances in the research of cytokine storm mechanism induced by Corona Virus Disease 2019 and the corresponding immunotherapies. *Zhonghua shao shang za zhi= Zhonghua shaoshang zazhi= Chinese journal of burns, 36*, E005-E005.

Cheung, A., Tu, L., Macnab, A., Kwon, B. K., & Shadgan, B. (2022). Detection of hypoxia by near-infrared spectroscopy and pulse oximetry: a comparative study. *Journal of Biomedical Optics, 27*(7), 077001.

Elas, M., Krzykawska-Serda, M., Gonet, M., Kozińska, A., & Płonka, P. M. (2019). Electron Paramagnetic Resonance Imaging-Solo and Orchestra *Medical Imaging Methods* (pp. 1-42): Springer.

Jiang, X., Bian, G.-B., & Tian, Z. (2019). Removal of artifacts from EEG signals: a review. *Sensors, 19*(5), 987.

Kalid, N., Zaidan, A., Zaidan, B., Salman, O. H., Hashim, M., & Muzammil, H. (2018). Based real time remote health monitoring systems: A review on patients prioritization and related" big data" using body sensors information and communication technology. *Journal of medical systems, 42*(2), 1-30.

Liu, S.-H., Liu, H.-C., Chen, W., & Tan, T.-H. (2020). Evaluating quality of photoplethymographic signal on wearable forehead pulse oximeter with supervised classification approaches. *IEEE Access, 8*, 185121-185135.

Metcalfe, B., Iravani, P., Graham-Harper-Cater, J., Bowman, R., Stirling, J., & Wilson, P. (2021). A cost-effective pulse oximeter designed in response to the COVID-19 pandemic. *Journal of Open Hardware, 5*(1).

Nitzan, M., Nitzan, I., & Arieli, Y. (2020). The various oximetric techniques used for the evaluation of blood oxygenation. *Sensors, 20*(17), 4844.

Panneer, S., Kantamaneni, K., *et al.* (2022). *Health, economic and social development challenges of the COVID-19 pandemic: Strategies for multiple and interconnected issues.* Paper presented at the Healthcare.

Tamura, T., Maeda, Y., Sekine, M., & Yoshida, M. (2014). Wearable photoplethysmographic sensors—past and present. *Electronics, 3*(2), 282-302.

Tarvirdizadeh, B., Golgouneh, A., Tajdari, F., & Khodabakhshi, E. (2020). A novel online method for identifying motion artifact and photoplethysmography signal reconstruction using artificial neural networks and adaptive neuro-fuzzy inference system. *Neural Computing and Applications, 32*(8), 3549-3566.

Tsiakaka, O., Gosselin, B., & Feruglio, S. (2020). Source–detector spectral pairing-related inaccuracies in pulse oximetry: Evaluation of the wavelength shift. *Sensors, 20*(11), 3302.

Utomo, B., Luthfiyah, S., Mudjiono, U., & Hamzah, T. (2019). *The real-time vital sign monitor for heart rate and spo2 parameter using internet of things technology.* Paper presented at the Journal of Physics: Conference Series.

van der Kooij, K. M., & Naber, M. (2019). An open-source remote heart rate imaging method with practical apparatus and algorithms. *Behavior research methods, 51*(5), 2106-2119.

Vidakis, K., Mavrogiorgou, A., Kiourtis, A., & Kyriazis, D. (2020). *A comparative study of short-range wireless communication technologies for health information exchange.* Paper presented at the 2020 International conference on electrical, communication, and computer engineering (ICECCE).

Schematic Diagram of the Pulse Oximeter Model

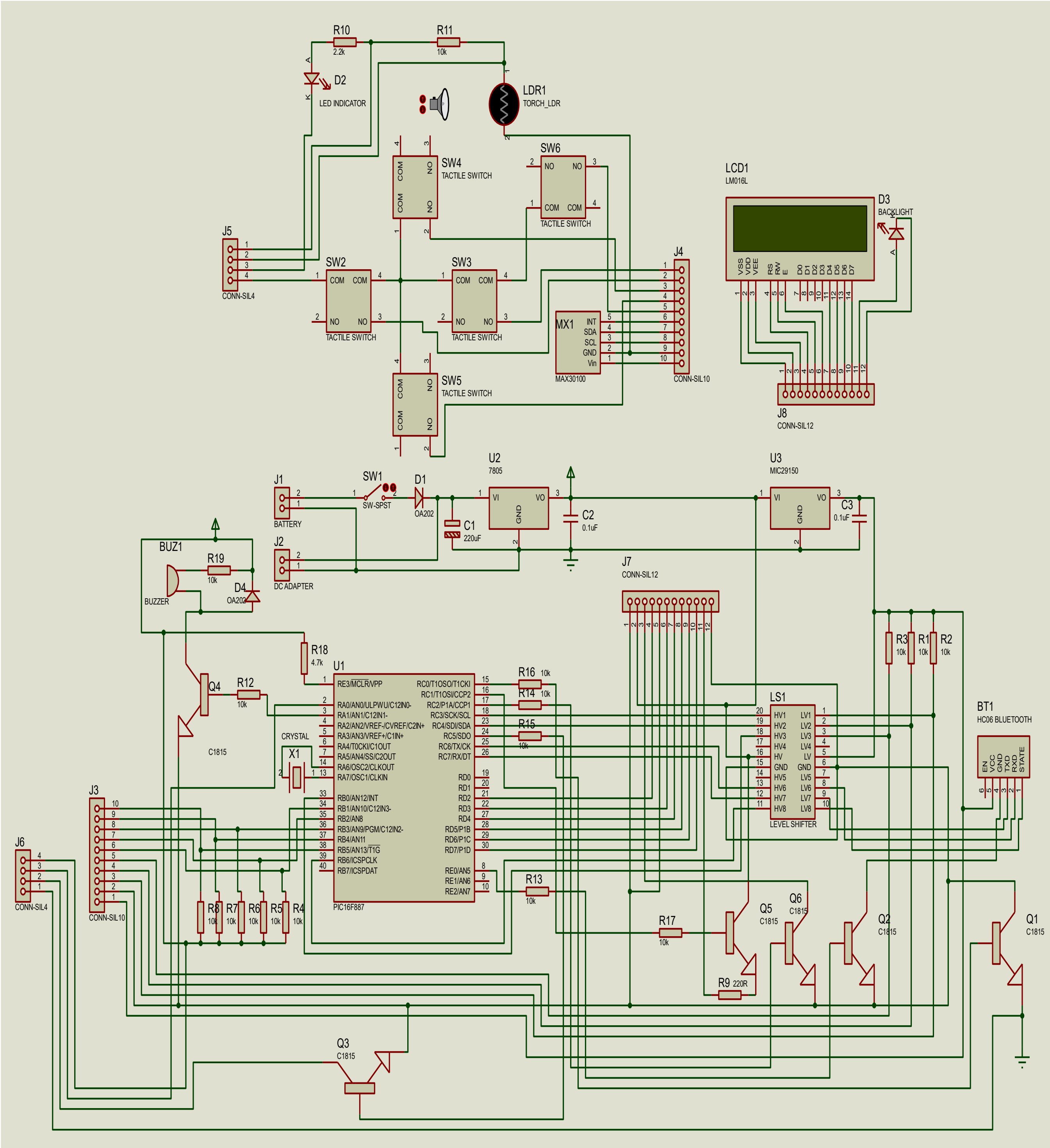
R10
2.2k
R11
10k
D2
LED INDICATOR
LDR1
TORCH_LDR
SW4
TACTILE SWITCH
SW6
TACTILE SWITCH
LCD1
LM016L
D3
BACKLIGHT
J5
CONN-SIL4
SW2
TACTILE SWITCH
SW3
TACTILE SWITCH
J4
CONN-SIL10
MX1
MAX30100
INT
SDA
SCL
GND
Vin
SW5
TACTILE SWITCH
J8
CONN-SIL12
VSS VDD VEE RS RW E D0 D1 D2 D3 D4 D5 D6 D7
J1
BATTERY
SW1
SW-SPST
D1
OA202
U2
7805
C1
220uF
C2
0.1uF
U3
MIC29150
C3
0.1uF
J2
DC ADAPTER
BUZ1
BUZZER
R19
10k
D4
OA202
J7
CONN-SIL12
R18
4.7k
U1
Q4
C1815
R12
10k
CRYSTAL
X1
R16
10k
R14
10k
R15
10k
R3
R1
R2
10k
LS1
LEVEL SHIFTER
BT1
HC06 BLUETOOTH
EN VCC GND TXD RXD STATE
RE3/MCLR/VPP
RA0/AN0/ULPWU/C12IN0-
RA1/AN1/C12IN1-
RA2/AN2/VREF-/CVREF/C2IN+
RA3/AN3/VREF+/C1IN+
RA4/T0CKI/C1OUT
RA5/AN4/SS/C2OUT
RA6/OSC2/CLKOUT
RA7/OSC1/CLKIN
RB0/AN12/INT
RB1/AN10/C12IN3-
RB2/AN8
RB3/AN9/PGM/C12IN2-
RB4/AN11
RB5/AN13/T1G
RB6/ICSPCLK
RB7/ICSPDAT
RC0/T1OSO/T1CKI
RC1/T1OSI/CCP2
RC2/P1A/CCP1
RC3/SCK/SCL
RC4/SDI/SDA
RC5/SDO
RC6/TX/CK
RC7/RX/DT
RD0
RD1
RD2
RD3
RD4
RD5/P1B
RD6/P1C
RD7/P1D
RE0/AN5
RE1/AN6
RE2/AN7
PIC16F887
HV1 HV2 HV3 HV4 HV GND HV5 HV6 HV7 HV8
LV1 LV2 LV3 LV4 LV GND LV5 LV6 LV7 LV8
J3
CONN-SIL10
J6
CONN-SIL4
R8 R7 R6 R5 R4
10k
R13
10k
R17
10k
R9 220R
Q5
C1815
Q6
C1815
Q2
C1815
Q1
C1815
Q3
C1815